Available online at www.sciencedirect.com
ScienceDirect
Biochemical and Biophysical Research Communications 363 (2007) 82–88
BBRC
www.elsevier.com/locate/ybbrc

LIV-1 suppression inhibits HeLa cell invasion by targeting ERK1/2-Snail/Slug pathway

Le Zhao [a], Wei Chen [a], Kathryn M. Taylor [b], Bin Cai [a], Xu Li [a,*]

[a] Center for Laboratory Medicine, The First Affiliated Hospital, School of Medicine, Xi'an Jiaotong University, Xi'an, China
[b] Tenovus Centre for Cancer Research, Welsh School of Pharmacy, Cardiff University, UK

Received 13 August 2007
Available online 30 August 2007

Abstract

It was reported that expression of the estrogen-regulated zinc transporter LIV-1 was particularly high in human cervical cancer cell line HeLa. This result prompted us to study the role that LIV-1 played in human cervical cancer. The results of real-time PCR showed that LIV-1 mRNA was significantly higher in cervical cancer in situ than in normal tissues. RNAi mediated suppression of LIV-1 in HeLa cells significantly inhibited cell proliferation, colony formation, migration, and invasive ability, but had no effect on cell apoptosis. Furthermore, LIV-1 suppression is accompanied by down-regulation of p44/42 MAPK, phospho-p44/42 MAPK, Snail and Slug expression levels. Hence, our data provide the first evidence that LIV-1 mRNA is overexpressed in cervical cancer in situ and is involved in invasion of cervical cancer cells through targeting MAPK-mediated Snail and Slug expression.

Keywords: Cervical carcinoma; Epithelial–mesenchymal transition; LIV-1; MAPK; Snail; Slug

Cervical carcinoma is now the second leading cause of cancer-related deaths in women worldwide [1]. Although the wide use of Papanicolaou smear screening has led to a decline in mortality from cervical cancer, many patients still died of cancer metastasis. Therefore, it is urgent to elucidate the mechanisms involved in cervical cancer metastasis.

A growing body of evidence supports the idea that epithelial–mesenchymal transition (EMT), where epithelial cells acquire mesenchymal gene-expression patterns and phenotypic traits, plays a critical role in the metastatic process of cancers [2,3]. EMT was first recognized as a feature of embryogenesis in the early 1980s and was found to participate in mesoderm and neural crest formation during normal development. Recently, more and more observations strongly suggest that EMT is an important event in the progression of many carcinomas as well [4,5]. Therefore, genes that regulate EMT are now attracting increasing attention as inducers of cancer progression.

Zinc finger transcription factor Snail is important EMT regulators [6]. During development, Snail is involved in the ingression of the early mesodermal cells at gastrulation and in the delamination of the neural crest from the neural tube. It is also involved in the EMT that takes place concomitant with the acquisition of invasive properties in tumors [7,8]. Its up-regulation was found in ovarian cancer, breast cancer, gastric cancer, colon cancer, etc., and was associated with metastasis [9–12]. Recent work linked zinc transporter LIV-1 and Snail in controlling EMT in zebrafish gastrula organizer and supposed LIV-1 to be a potential regulator of EMT [13]. LIV-1, a member of the ZIP family of zinc transporters, is an integral plasma membrane protein that transports zinc into cells. LIV-1 expression in HeLa cells was particularly high, but its significance was unclear [14]. The aim of our study was to investigate its role in the progression of cervical neoplasia.

* Corresponding author.
E-mail address: lixu56@mail.xjtu.edu.cn (X. Li).

0006-291X/$ - see front matter © 2007 Elsevier Inc. All rights reserved.
doi:10.1016/j.bbrc.2007.08.127

Materials and methods

Tissue samples. The study was approved by the Ethics Committee of the First Affiliated Hospital, School of Medicine of Xi'an Jiaotong University, informed consent was obtained from each patients. All specimens were collected at the First Affiliated Hospital of Medical School, Xi'an Jiaotong University from February 2004 to August 2006. Cancer tissues were taken from 61 cases of primary cervical cancer who not subjected to chemo- or radiotherapy before undertook surgical resection or biopsy. Histopathological examination indicated that all cancer tissues were squamous carcinomas and that at least 80% of tumor cells presented. Adjacent normal cervical tissues from 18 cases of cervical cancer displayed no histological abnormalities were used as controls. All tissue samples were immediately snap-frozen in liquid nitrogen and stored at −80 °C until used for analysis. The age of the patients ranged from 28 to 69 (average 45.7 ± 8.7 years). The clinical and histopathological information of all patients are showed in Table 1.

Real-time PCR analysis. Total RNAs were extracted from frozen tissue samples or cultured cells using TRIzol® reagent (Invitrogen Life Technologies, Carlsbad, CA, USA) according to the manufacture's protocol. RNA concentration and purity were determined on a UV spectrophotometer (BioRad Inc., Hercules, CA, USA) by the 260 nm absorbance and 260–280 nm absorbance ratio, respectively. cDNA synthesis was conducted using SYBR® ExScript™ RT-PCR Kit (Takara Biotechnology Co. Ltd., Dalian, China) according to manufacturer's instructions: 500 ng total RNA was mixed with 2 μl of 5× ExScript™ RTase buffer, 0.5 μl of dNTP mixture, 0.5 μl of random 6 mers, 0.25 μl of ExScript™ RTase and 0.25 μl of RNase Inhibitor in a total volume of 10 μl. The reactions were performed at 42 °C for 12 min, followed by inactivation of the reverse transcriptase at 95 °C for 2 min. The cDNA was stored at −20 °C.

Quantitative real-time RT-PCR for the LIV-1 mRNA was performed on an ABI PRISM® 7300 Sequence Detection System (Applied Biosystems, Foster City, CA, USA) using SYBR Green Master Mix (Takara Biotechnology Co. Ltd., Dalian, China). For normalization the gene GAPDH was used. Final reaction volume is 25 μl, containing 12.5 μl 2× SYBR® Premix Ex Taq™, 1.0 μl each primer (10 μM), 0.5 μl 50× ROX reference dye and 1.0 μl cDNA. Cycling conditions were as follows: initial denaturation at 95 °C for 10 s, followed by 40 cycles of 95 °C for 5 s and 59 °C for 31 s. Each measurement was performed in triplicate, and no-template controls were included for each assay. After PCR, a dissociation curve analysis was done. Relative gene expression was calculated using the $2^{-\Delta\Delta CT}$ method with pooled cDNA from all samples as a reference [15]. All oligonucleotide primers were designed and synthesized by Takara (Dalian, China). The primer sequences are listed as follows:

Gene length	Primer sequence	Position (mRNA)	Product (bp)
GAPDH (NM_004360)	F 5′-AGGTCGGAGT CAACGGATTTG-3′	66–86	551
	R 5′-GTGATGGCAT GGACTGTGGT-3′	597–616	
LIV-1 (NM_012319)	F 5′-GGTGATGGCCT GCACAATTTC-3′	1923–1943	161
	R 5′-TTAACGGTCAT GCCAGCCTTTAGTA-3′	2059–2083	

F, forward primer; R, reverse primer.

Cell culture. Human cervical cancer cell line HeLa was cultured in RPMI 1640 medium (Gibco-BRL, Gaithersburg, MD, USA) supplemented with 10% bovine calf serum, 100 U/ml penicillin, and 100 μg/ml streptomycin. Cultures were maintained at 37 °C in a humidified atmosphere with 5% CO_2.

RNAi. Three shRNA insert sequences for LIV-1, which were designed by using the software siRNA Construct Builder (GenScript Corp., Piscataway, NJ, USA), were as follows: 5′-gatccAGGCTGGCATGACCGTTAAttcaagagaTTAACGGTCATGCCAGCCTttttttggaaa-3′, 5′-gatccTGAGTTGCCTCATGAATTAttcaagagaTAATTCATGAGGCAACTCAttttttggaaa-3′, and 5′-gatccCTCAGATAGTTCAGGTAAAttcaagagaGATTTACCTGAACTATCTGAGttttttggaaa-3′. As a negative control, a mock vector was also designed, whose inserted sequence was 5′-gatccTTCTCCGAACGTGTCACGTttcaagagaACGTGACACGTTCGGAGAAttttttggaaa-3′ (scrambled) which does not have any target region in human genes. Sense and antisense oligonucleotides were annealed and subcloned into the shRNA expression vector pRNAT-U6.1/Neo (GenScript Corp., Piscataway, NJ, USA). The resultant plasmids were designated pRNAT-U6.1/Neo-LIV1, pRNAT-U6.1/Neo-LIV2, pRNAT-U6.1/Neo-LIV3, and pRNAT-U6.1/Neo-Neg, respectively. Plasmid DNA was extracted from *Escherichia coli* transformants using Fastfilter Endo-free Plasmid Midi Kit (Omega Bio-Tek Inc., Doraville, GA, USA).

Transfection experiment was conducted using Lipofectamine 2000 reagent (Invitrogen; Carlsbad, CA, USA) according to the manufacturer's instruction. HeLa cells were selected with 400 μg/ml G418 (Gibco-BRL, Gaithersburg, MD, USA) for 1 week and then maintained in normal 1640 medium containing 200 μg/ml G418. Individual clones were picked, based on GFP expression and neomycin resistance.

Western blot analysis. Cells were lysed with RIPA buffer (150 mM NaCl, 1.0% Nonidet P-40, 0.5% sodium deoxycholate, 0.1% SDS, 50 mM Tris, pH 8.0) containing protease inhibitor cocktail (Roche Applied Science, Mannheim, Germany) and 2 mM sodium vanadate. Protein concentration was determined by BCA protein assay reagent kit (Pierce, Rockford, IL, USA). Equal amounts of cell lysates were separated by 10% SDS–PAGE, electrophoretically transferred to nitrocellulose membrane (Pall, Pensacola, FL, USA), immunoblotted with primary antibody against LIV-1, p44/42 MAPK, phospho-p44/42 MAPK (Cell Signaling Technology, Danvers, MA, USA) or β-actin (Biosynthesis Biotechnology, Beijing, China). Anti-LIV-1 antibody was kindly provided by Dr. Kathryn M. Taylor, Tenovus Centre for Cancer Research, Welsh School of Pharmacy, Cardiff University. Blots were visualized with anti-rabbit or anti-mouse IgG conjugated with peroxidase (HRP) and ECL reagents (Pierce, Rockford, IL, USA).

Cell proliferation, cell cycle, and colony formation assay. Cell proliferation was assessed using Monotetrazolium (Amresco, Solon, OH, USA) assays. Briefly, the cells were separately seeded at the same time into 96-well culture plates and then routinely cultured for 6 days. 0.5 mg/ml MTT was added to each well. The cells were cultured at 37 °C for 4 h, 150 μl DMSO was added, and the 490 nm wave-length absorption value (*A* value) was measured at 1, 2, 3, 4, 5 and 6 day after seeding of cells. All experiments were performed in triplicate and repeated three times.

Cell cycle analysis was conducted as follows: cells were collected, washed twice with PBS, and fixed with ice-cold 70% ethanol for at least 1 h. The fixed cells were washed and stained with propidium iodide (Beckman Coulter, FL, USA). After incubation for 30 min at 37 °C, samples were analyzed by a flow cytometry (Beckman Coulter, FL, USA). Cell cycle analysis of DNA histograms was performed with Multi cycle software.

Colony formation was assessed as follows: cells were trypsinized into a single cell suspension. A total of 100 cells were plated in each well of 6-well plates and kept for 14 days in RPMI 1640 supplemented with 10% bovine calf serum containing G418 to allow colony formation. The colonies were fixed in methyl alcohol and stained with Giemsa (Gibco-BRL, Gaithersburg, MD, USA). Cell clones over 50 cells were counted using a grid. Three independent experiments were performed.

Table 1
LIV-1 mRNA expression in normal cervical tissue and cervical carcinoma

Type	Cases	LIV-1 mRNA level	*P* value[a]
Normal cervical tissue	18	0.82 ± 0.51	
Cervical carcinoma in situ	7	7.86 ± 7.04	0.009
Cervical carcinoma	54	1.68 ± 1.32	

[a] ANOVA analysis. Multiple comparisons: cervical carcinoma in situ vs normal cervical tissue, $P = 0.006$; cervical carcinoma vs normal cervical tissue, $P = 0.788$; cervical carcinoma in situ vs cervical carcinoma, $P = 0.008$.

Apoptosis assay. Apoptosis was monitored by measuring nuclear condenses by Hoechst 33258 staining. Cells grown on glass coverslips were fixed with 4% paraformaldelyde for 20 min at room temperature, and then washed and stained with 167 mM Hoechst 33258 at 37 °C for 30 min. Slides were observed using a fluorescence microscope.

Furthermore, Bcl-2 and Bax protein expression was detected with immunocytochemistry. Briefly, cells grown on glass coverslips were fixed with 4% paraformaldelyde, incubated with 3% hydrogen peroxide for 10 min to quench endogenous peroxidase activity, and permeabilized with 0.1% Triton X-100 for 10 min. After blocking with nonimmune serum, mouse anti-bcl-2 or mouse anti-bax (working solution, Zhongshan, Beijing, China) primary antibody was added overnight at 4 °C, followed by addition of biotinylated secondary antibody and avidin–biotin horseradish peroxidase complex. Bound peroxidase was detected by addition of substrate DAB and hematoxylin counterstaining. Slides were mounted and examined under a microscope (Olympus, Japan).

Cell invasion and motility assay. Invasion assay was done in a 24-well Millicell chamber. The 8-μm pore inserts were coated with 15 μg of Matrigel (Becton Dickinson Labware, Bedford, MA). 5×10^5 cells were added to coated filters in 100 μl of serum-free medium in triplicate wells. Five hundred microliters of RPMI 1640 media containing 20% fetal bovine serum was added to the lower chamber as chemoattractant. After 24 h at 37 °C in a 5% CO_2 incubator, the Matrigel coating on the upper surface of the filter was wiped off using a cotton swab. Cells that migrated through the filters were fixed in 2.5% glutaraldehyde for 30 min, stained with Giemsa, photographed, and counted.

The motility assay was conducted in a similar fashion without coating with Matrigel. 1×10^6 cells in 100 μl serum-free 1640 medium were seeded in the upper chamber of Milllicell inserts. The plates were incubated for 8 h at 37 °C in a 5% CO_2 incubator, then the cells in the lower wells were fixed, stained, and counted. Each experiment was carried out in triplicate.

Immunohistochemistry. Immunohistochemistry was performed as described above with goat anti-Snail or anti-Slug (1:200, Santa Cruz, CA, USA) primary antibody. Immunolabelling was performed by a standard Avidin–Biotin (ABC) technique using a commercial kit (Maxim, China). Slides were examined under a microscope at a magnification of 200×.

Statistical analysis. All statistical analyses were performed using the SPSS13.0 software. The results were presented as means ± SD of three replicate assays. Differences between different groups were assessed using ANOVA or Dunnett *t*-test. A P value of <0.05 was considered to indicate statistical significance.

Results

Expression of LIV-1 in cervical cancer and normal cervical tissues

The transcription level for LIV-1 was significantly higher in cervical cancer in situ compared to normal tissues (7.86 ± 7.04 vs 0.82 ± 0.51, Dunnett *t*-test, $P = 0.006$) and invasive cancer (7.86 ± 7.04 vs 1.68 ± 1.32, Dunnett *t*-test, $P = 0.0008$; Table 1). But no difference was detected between normal tissues and invasive cancer tissues ($P = 0.788$) and no significant correlation was identified between LIV-1 expression and clinicopathologic paramers ($P > 0.05$; Table 2) (See Fig. 1).

Down-regulation of LIV-1 by transfection with pRNAT-u6.1/Neo encoding a LIV-1 shRNA

We developed pRNAT-U6.1/Neo vectors containing small hairpin constructs capable of generating 19-nucleotide duplex RNAi oligonucleotides corresponding to LIV-

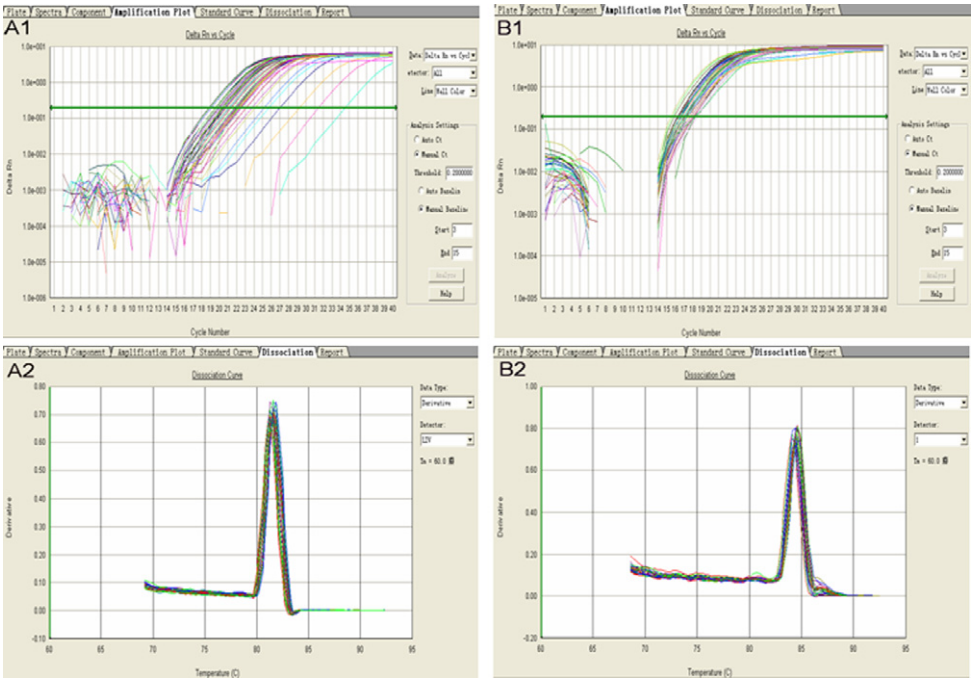

Fig. 1. Real-time amplification plots for LIV-1 (A1) and GAPDH (B1) genes. The vertical axis represents Delta Rn, which is the normalized intensity of fluorescence of the reporter dye (SYBR Green I), representing the amount of amplicons. The horizontal axis represents the number of PCR cycles. The horizontal line represents the threshold cycle (the cycle number at which the fluorescence reaches the threshold value). Dissociation curves for LIV-1(A2) and GAPDH (B2) PCR reactions. Dissociation curves provide a graphical representation of the PCR product after the amplification process. A single peak in positive samples suggests a single size product.

Table 2
Relationship between LIV-1 mRNA expression and clinicopathological characteristics of cervical carcinoma

Item	Cases	LIV-1 mRNA level	*P* value
Age (years)			
50	43	12.69 ± 4.05	0.283
>50	18	8.92 ± 6.59	
FIGO stage			
I	14	1.44 ± 1.00	0.434
II	33	1.87 ± 1.51	
III	7	1.30 ± 0.75	
Histological grade			
Well differentiated	5	0.49 ± 0.16	0.097
Moderately differentiated	34	1.86 ± 1.36	
Poorly differentiated	15	1.68 ± 1.29	
Invasion depth			
<1/3	16	1.82 ± 1.50	0.612
⩾1/3	38	1.62 ± 1.25	
Lymph node metastasis			
Positive	19	1.42 ± 1.03	0.296
Negative	35	1.82 ± 1.45	

1. After LIV-1 shRNA transduction, cell sorting was carried out by selecting cells expressing the GFP marker and neomycin resistance. The resulted sublines stably integrated with pRNAT-U6.1/Neo-LIV1, pRNAT-U6.1/Neo-LIV2, pRNAT-U6.1/Neo-LIV3 or pRNAT-U6.1/Neo-Neg were designated as pRNAT-H1, pRNAT-H2, pRNAT-H3, and pRNAT-HN, respectively (Fig. 2A–D). Real-time PCR and Western blotting analysis indicated that LIV-1 mRNA and protein level were reduced in pRNAT-H1 compared with that in pRNAT-HN (Fig. 2E–F). LIV-1 mRNA and protein level in pRNAT-H2 and pRNAT-H3 were not significantly different from those of pRNA-HN.

RNAi of LIV-1 in HeLa cells impairs cell proliferation

The effect of LIV-1 protein reduction on HeLa cell proliferation was examined using the MTT assay. As shown in Fig. 3A, the cell proliferation of LIV-1-knockdown subline (pRNAT-H1) was reduced compared with the control cell line (pRNAT-HN). The suppression effect became obvious from the fifth day, and the difference was significant between pRNAT-H1 and pRNAT-HN ($P < 0.01$).

We subsequently assessed cell cycle progression by flow cytometry. Compared to the control cells pRNAT-HN, there was a increase in the relative number of cells in G1 phase (66.55% vs 59.3%) and a decrease in S-phase cells (18.05% vs 27.05%), but the differences were not significant (Fig. 3B).

In addition to reduction in cell proliferation, pRNAT-H1 also demonstrated a decrease in colony formation. After 14 days culture, the colonies that pRNAT-H1 formed was 16.7% of pRNAT-HN (Fig. 3C).

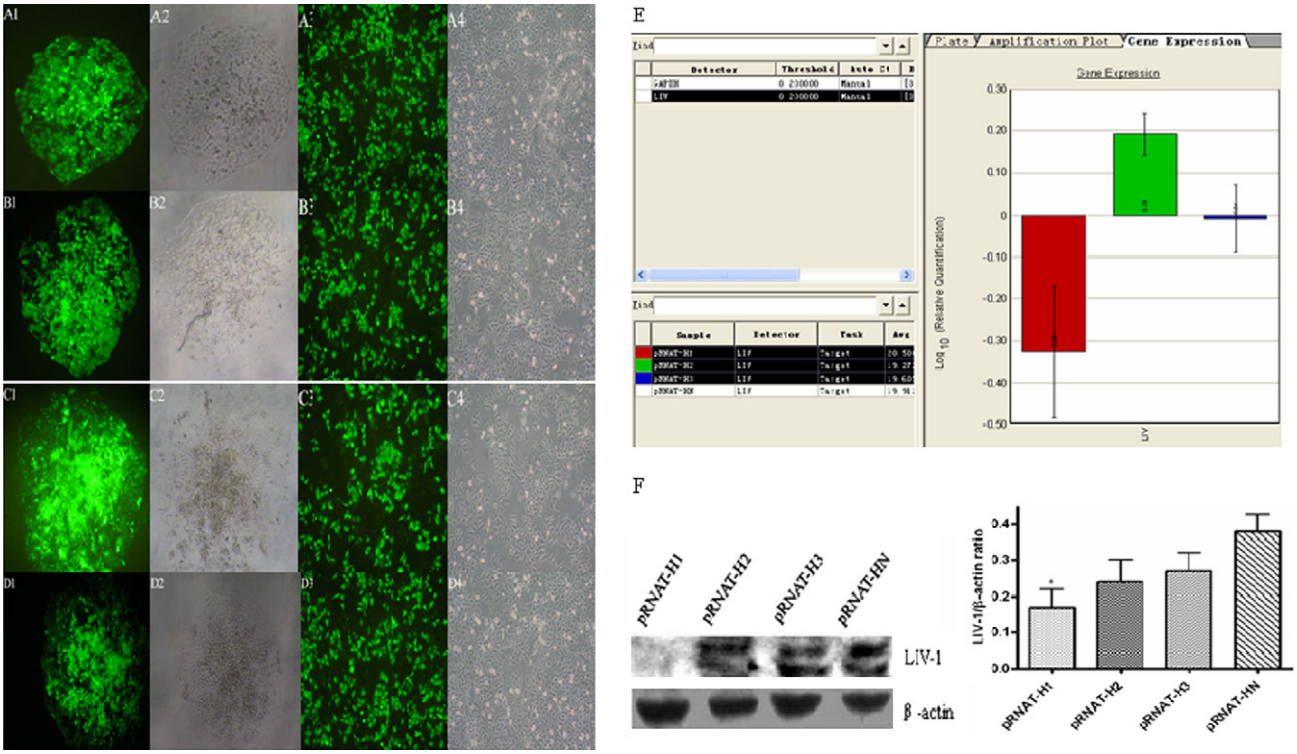

Fig. 2. (A1–D1) Green fluorescent image of cell clone stably integrated with the plasmid pRNAT-U6.1/Neo-LIV1, pRNAT-U6.1/Neo-LIV2, pRNAT-U6.1/Neo-LIV3, and pRNAT-U6.1/Neo-Neg, respectively. (A2–D2) Bright field microscopic image corresponding to A1, B1, C1, and D1, respectively. (A3–D3) Green fluorescent image of each cell clone after amplification. (A4–D4) Bright field microscopic image corresponding to A3, B3, C3, and D3, respectively. Original magnification 100×. (E) Real-time PCR analysis showed that LIV-1 mRNA expression was reduced in pRNAT-H1 cells, compared to that of pRNAT-HN cells. GAPDH was used as an internal control. (F) Western blot analysis indicated LIV-1 protein level was suppressed in pRNAT-H1 compared to that of pRNAT-HN cells. β-Actin was used as loading control.

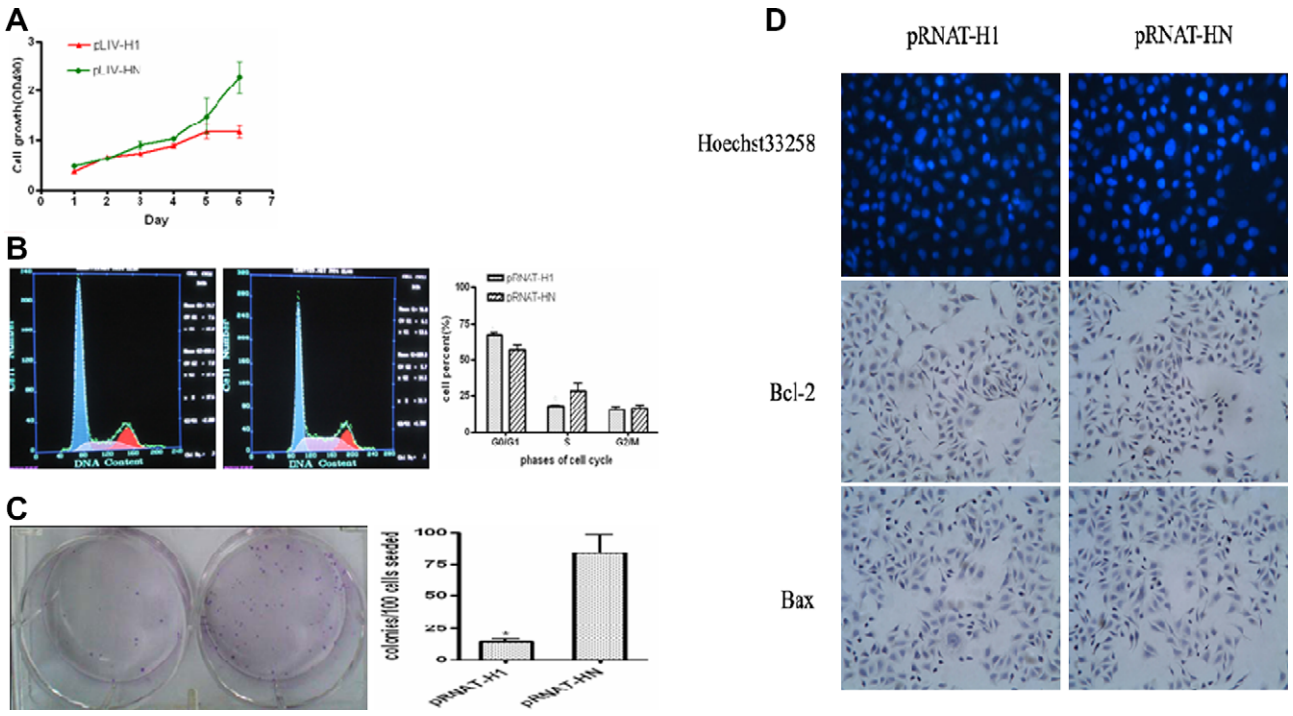

Fig. 3. Growth suppression of HeLa cells by LIV-1 down-regulation. (A) MTT assay was used to assess the effect of LIV-1 down-regulation on growth of HeLa cells in vitro. Compared to pRNAT-HN cells, pRNAT-H1 showed inhibition of cell growth. Results represented mean of three independent experiments performed in triplicates. (B) Distribution of cell cycle phases in HeLa cells. The relative number of cells in G1 phase was increased and the cells in S phase was decreased in pRNAT-H1 cells compared with pRNAT-HN. (C) Colony formation assay. Representative cultures of pRNAT-H1 cells (left well) compared to pRNAT-HN cells (right well) are shown. Values represent means ± SD of at least three independent experiments. $^{*}P < 0.05$ indicates that values for pRNAT-H1 cells were statistically significantly different from those for pRNAT-HN cells. (D) Apoptosis assay. Hoechst 33258 nuclear staining showed that nearly no apoptosis was detected both in pRNAT-H1 and pRNAT-HN. Immunocytochemical staining of Bcl-2 and Bax showed that both pRNAT-H1 and pRNAT-HN cells displayed negative for Bcl-2 and Bax.

Cell apoptosis detection

Hoechst 33258 staining was used to detect cell apoptosis. Most of nuclei displayed dispersal uniform fluorescence (Fig. 3D) which indicated normal nuclei, suggesting few apoptosis occurred in cells expressed stably with LIV-1 shRNA and control plasmid. To demonstrate the result, we further examined the anti-apoptotic protein Bcl-2 and the proapoptotic protein Bax expression with immunohistochemistry technique, and we found both pRNAT-H1 and pRNA-HN were negative for Bcl-2 and Bax (Fig. 3D). These data therefore demonstrated that the reduction of LIV-1 level did not affect cell apoptosis.

Effect of LIV-1 suppression on cell motility and invasion

To study the effect of LIV-1 suppression on cell migration, pRNAT-HN, and pRNAT-H1 cells were seeded on Millicell chambers with uncoated filters. After 8 h of incubation, the motility potential of pRNAT-H1 cells was strongly inhibited (Fig. 4A; $P < 0.05$).

The in vitro invasion assay was designed to test whether LIV-1 down-regulation altered the invasive potential of tumor cells in Matrigel-coated Milliwell chamber. The invasive potential of pRNAT-H1 cells appeared significantly reduced (Fig. 4A; $P < 0.05$).

Inhibition of LIV-1 expression by LIV-1 shRNA downregulates Snail and Slug in HeLa cells

We further examined the Snail and Slug protein level in pRNAT-H1 and pRNAT-HN cells by immunohistochemistry assay. As shown in Fig. 4B, there was significant reduction of Snail and Slug staining in the nuclei and cytoplasm of the pRNAT-H1 compared to pRNAT-HN control cells. To understand whether p42/44 MAPK mediated the LIV-1 regulation of SNAI1/2, we examined the protein level of p44/42 MAPK and phospho-p44/42 MAPK using Western blot, and we did find that both of them downregulated in pRNAT-H1 cells (Fig. 4C).

Discussion

Essential for embryonic development, epithelial–mesenchymal transition also occurs during cancer progression. The transcriptional repressors, Snail and Slug, are expressed in regions where EMT occurs during development, such as neural crest. Increasing studies indicated that Snail and Slug played important role in EMT of cancer cells. While recent study suggests a link between zinc transporter LIV-1 and Snail in controlling EMT during zebrafish embryogenesis. In the present study, we assessed the implication of LIV-1 in cervical cancer.

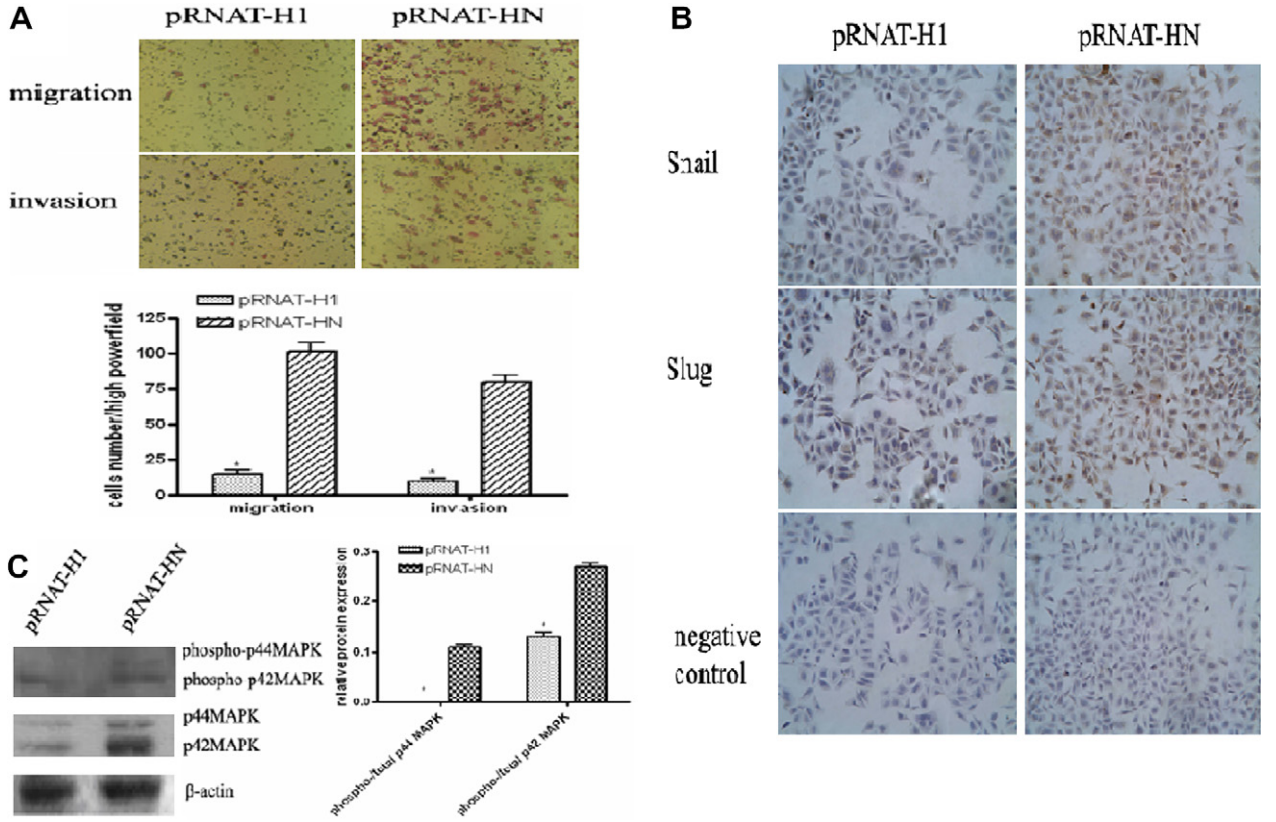

Fig. 4. (A) RNAi knockdown of LIV-1 expression inhibits the motility and invasive potential of HeLa cells. Representative number of motility or invading cells was counted under the microscope in three random fields at 200×. Significant difference from pRNAT-HN control cells is indicated by asterisks ($P < 0.05$). Results are representative of three separate experiments. Representative visual field of pRNAT-H1 cells (left well) compared to pRNAT-HN cells (right well) is shown. (B) Immunocytochemical assay of Snail and Slug protein expression. Snail and Slug expression were significantly reduced in pRNAT-H1 compared to pRNAT-HN. (C) Western blot analysis showed that both p44/42 MAPK and phospho-p44/42 MAPK protein level were suppressed in pRNAT-H1 compared to those of pRNAT-HN cells. β-Actin was used as loading control.

We constructed three sublines that stably expressed LIV-1 shRNA and one subline that express negative control shRNA. Results of real-time PCR and Western blot demonstrated that LIV-1 mRNA and protein were significantly suppressed only in one subline, i.e. pRNAT-H1, compared to pRNAT-HN control cells. Therefore, subsequent analysis was conducted using pRNATH1 and pRNAT-HN.

Since zinc is a pivotal element in all rapidly growing tissues because it is a component of DNA and RNA polymerase, and seems to have a modulatory and protective action for the growth of both normal and cancer cells. LIV-1, being an important Zinc transporter, may play a part in cell growth. Our data supported this presumption. The growth of pRNAT-H1 cells was significantly inhibited compared with pRANT-HN cells. And cell cycle analysis showed that in pRNAT-H1, G0/G1 cells were more and S-phase cells were less than pRNAT-HN cells, although no significance was found. In addition, colony formation was markedly impaired in pRNAT-H1 cells. These data suggest that LIV-1 is associated with HeLa cells growth. To investigate whether growth inhibition of pRNAT-H1 is resulted from cell apoptosis, we assayed cell apoptosis. Hoechst 33258 staining and Bcl-2 and Bax immunocytochemical staining consistently showed that there was almost no cell apoptosis in both pRNAT-H1 and pRANT-HN cells. Thus, we conclude that LIV-1 suppression has no effect on cell apoptosis.

LIV-1 was associated with estrogen-positive breast cancer and its metastatic spread to the regional lymph nodes [16]. Therefore, we subsequently analyzed change of cell migration and invasion potential after knockdown of LIV-1. As expected, pRNAT-H1 cells showed a substantial reduction in migration and matrigel invasion capacity, which indicated that LIV-1 expression was required for HeLa cell invasion as well as metastasis. LIV-1 suppression alone may cause the inhibition of cancer migration and invasion potential because LIV-1 contained a potential metalloprotease motif similar to that presented in the matrix metalloproteases [17]. But combined with the report that LIV-1 was an upstream regulator of Snail which was found to be involved in invasive property of cancer cells, we suppose that LIV-1 probably play this kind of role through down regulating Snail expression. Immunocytochemical analysis of Snail was therefore conducted. Because Slug is also belongs to Snail transcription factors family and was associated with cancer metastasis, we examined its expression at the same time. The results showed

that Snail and Slug expression were markedly reduced as a result of LIV-1 protein knockdown. It thus appears that LIV-1 may regulate Snail and Slug expression in HeLa cells, if it is the case, then whether LIV-1 regulates Snail and Slug expression directly or through other molecular? It was reported that Snail RNA levels were dependent on p4ERK signaling pathway [18]. We then assayed the protein level of p44/42 MAPK and phospho-p44/42 MAPK using Western blot, and we found that LIV-1 suppression was accompanied with down-regulation of p44/42 MAPK and phospho-p44/42 MAPK.

Taken together, our data showed that LIV-1 was overexpressed in cervical cancer in situ. LIV-1 suppression in HeLa cells limits cell growth, and prevents in vitro migration and invasion probably through inactivating p44/42 MAPK-Snail/Slug signaling pathway. We believe that our study is helpful to elucidate the precise role that LIV-1 plays in cancer progression.

References

[1] D.M. Parkin, F. Bray, J. Ferlay, et al., Estimating the world cancer burden: globocan 2000, Int. J. Cancer 94 (2001) 153–156.

[2] B. Boyer, A.M. Valles, N. Edme, Induction and regulation of epithelial mesenchymal transitions, Biochem. Pharmacol. 60 (2000) 1091–1099.

[3] M.A. Huber, N. Kraut, H. Beug, Molecular requirements for epithelial–mesenchymal transition during tumor progression, Curr. Opin. Cell Biol. 17 (2005) 548–558.

[4] J.P. Thiery, Epithelial–mesenchymal transitions in tumour progression, Nat. Rev. Cancer 2 (2002) 442–454.

[5] J.P. Thiery, Epithelial–mesenchymal transitions in development and pathologies, Curr. Opin. Cell Biol. 15 (2003) 740–746.

[6] Y. Grau, C. Carteret, P. Simpson, Mutations and chromosomal rearrangements affecting the expression of snail, a gene involved in embryonic patterning in *Drosophila melanogaster*, Genetics 108 (1984) 347–360.

[7] A. Cano, M.A. Perez-Moreno, I. Rodrigo, A. Locascio, M.J. Blanco, M.G. del Barrio, F. Portillo, M.A. Nieto, The transcription factor snail controls epithelial–mesenchymal transitions by repressing *E*-cadherin expression, Nat. Cell Biol. 2 (2000) 76–83.

[8] M.A. Nieto, The snail superfamily of zinc-finger transcription factors, Nat. Rev. Mol. Cell Biol. 3 (2002) 155–166.

[9] N.K. Kurrey, A. K, S.A. Bapat, Snail and Slug are major determinants of ovarian cancer invasiveness at the transcription level, Gynecol. Oncol. 97 (2005) 155–165.

[10] M.J. Blanco, G. Moreno-Bueno, D. Sarrio, A. Locascio, A. Cano, J. Palacios, M.A. Nieto, Correlation of snail expression with histological grade and lymph node status in breast carcinomas, Oncogene 21 (2002) 3241–3246.

[11] E. Rosivatz, I. Becker, K. Specht, E. Fricke, B. Luber, R. Busch, H. Hofler, K.F. Becker, Differential expression of the epithelial–mesenchymal transition regulators snail, SIP1, and twist in gastric cancer, Am. J. Pathol. 161 (2002) 1881–1891.

[12] H.K. Roy, T.C. Smyrk, J. Koetsier, T.A. Victor, R.K. Wali, The transcriptional repressor SNAIL is overexpressed in human colon cancer, Dig. Dis. Sci. 50 (2005) 42–46.

[13] S. Yamashita, C. Miyagi, T. Fukada, N. Kagara, Y.S. Che, T. Hirano, Zinc transporter LIVI controls epithelialmesenchymal transition in zebrafish gastrula organizer, Nature 429 (2004) 298–302.

[14] K.M. Taylor, H.E. Morgan, A. Johnson, L.J. Hadley, R.I. Nicholson, Structure–function analysis of LIV-1, the breast cancer-associated protein that belongs to a new subfamily of zinc transporters, Biochem. J. 375 (2003) 51–59.

[15] K.J. Livak, T.D. Schmittgen, Analysis of relative gene expression data using real-time quantitative PCR and the 2(−Delta Delta C(T)) method, Methods 25 (2001) 402–408.

[16] D.L. Manning, J.F. Robertson, I.O. Ellis, C.W. Elston, R.A. McClelland, J.M. Gee, R.J. Jones, C.D. Green, P. Cannon, R.W. Blamey, et al., Oestrogen-regulated genes in breast cancer: association of pLIV1 with lymph node involvement, Eur. J. Cancer 30A (1994) 675–678.

[17] K.M. Taylor, R.I. Nicholson, The LZT proteins; the LIV-1 subfamily of zinc transporters, Biochim. Biophys. Acta 1611 (2003) 16–30.

[18] M.J. Barbera, I. Puig, D. Dominguez, S. Julien-Grille, S. Guaita-Esteruelas, S. Peiro, J. Baulida, C. Franci, S. Dedhar, L. Larue, et al., Regulation of Snail transcription during epithelial to mesenchymal transition of tumor cells, Oncogene 23 (2004) 7345–7354.